ISSN : 0974 - 7486 Volume 8 Issue 8

Trade Science Inc.

Materials Science
An Indian Journal

Full Paper

MSAIJ, 8(8), 2012 [336-342]

A thermogravimetric and metallographic study of the high temperature oxidation of a binary nickel-chromium alloy in humidified air. Part II: Scale spallation at cooling

Patrice Berthod[1,2,*], Saidou Kane[2]

[1]Institut Jean Lamour (UMR 7198), Team 206 "Surface and Interface, Chemical Reactivity of Materials", B.P. 70239, 54506 Vandoeuvre-lès-Nancy, (FRANCE)

[2]University of Lorraine, F.S.T., B.P. 70239, 54506 Vandoeuvre-lès-Nancy, (FRANCE)

E-mail: Patrice.Berthod@univ-lorraine.fr

Received: 4th March, 2012 ; Accepted: 4th April, 2012

ABSTRACT

A Ni-25Cr binary alloy was subjected to oxidation at four high temperatures, comprised between 1000 and 1300°C during 48 hours in dry air and in air enriched in water vapour, with recording of the mass gain. The cooling parts of the obtained thermogravimetry curves were exploited to observe the occurrence or not of scale spallation and the temperatures of spallation start if this happens. The oxides formed were observed after test by electronic and optical microscopy, and characterized by X-Ray Diffraction and image analysis. By comparison with dry air, the water concentration tried in this work induced a finer structure of the oxides scales formed during the isothermal stage, and a better resistance of these oxides against spallation when temperature decreases.

KEYWORDS

Nickel alloy;
Chromium;
Water vapour;
High temperature;
Scale spallation at cooling.

INTRODUCTION

Water vapour is often present in the hot oxidant gases in which pieces made of superalloys are working, as turbine blades in power generation processes or in aircraft motors[1]. The fact that these hot atmospheres are humidified may lead to changes for the mechanisms of high temperature oxidation[2], with notably consequences about the oxidation kinetics or the rates of volatilization of the oxides usually protecting alloys, alumina, silica or chromia, by formation of gaseous oxy-hydroxydes species. Especially concerning this later protective oxide, a great part of studies deal more with Fe-Cr alloys[3,4] than with nickel-based alloys, even if several works have been done recently about binary Ni-Cr alloys[5] and superalloys[6,7].

In the present work, which was carried out in the case of a binary Ni-25Cr cast alloy concerning the effect of humidity on the high temperature oxidation in conditions of varying temperature, after having examined in the first part the differences of behaviour which may occur during heating at a constant rate, the oxide spallation during the cooling, at constant rate too, will be here studied by following similar criteria as earlier studies[8-10] (exploitation of the thermogravimetric files) as well as by characterizing the oxides remaining on the samples in terms of nature, morphology and surface percentage.

EXPERIMENTAL

Thermogravimetry tests and exploitation of the cooling parts of the varying mass curves

One can remind that the alloys were synthesized by foundry from nickel and chromium (purity > 99.9 wt.%), under inert atmosphere. The samples were cut in the ingots (all of about 40g) with dimensions of about 10 × 10 × 3 mm^3, and polished with SiC-papers up to the 1200-grit SiC. The oxidation tests in dry air and in wet air were carried out in the same SETARAM Setsys thermo-balance coupled with a humidity generator SETARAM Wetsys, with circulation, at 20mL min^{-1}, of not humidified air (dry air) or of air enriched in water vapour to correspond to a Relative Humidity of 80% at 40°C (wet air). Four stage temperatures were considered: 1000, 1100, 1200 and 1300°C for a same duration - 48 hours - for the two atmospheres. At the end of the isothermal stage the oxidized samples were cooled at a constant rate (-5°C min^{-1}). Notably because of the difference of thermal expansion or contraction behavior usually observed between the metallic substrate and the oxide scale formed at high temperature on its surface, the latter one may endure increasing compression stresses which may lead to its local detachment. The occurrence of oxide spallation was studied by examining the cooling parts of the thermogravimetry curves as done in previous studies[8-10].

Outside examination of the oxidized samples

After the oxidation tests the samples were subjected to X-Ray Diffraction analysis to specify the number and natures of the oxides present on surface. This was performed using a Philips X'Pert Pro diffractometer (Cu K_α, wavelength: 1.54056 Å). The surface textures of the oxide scales were also observed using a Jeol JSM-7600F FEG-SEM (Field Emission Gun - Scanning Electron Microscope) in Secondary Electrons mode. The oxidized samples were further scanned (Canon CanoScan Lide35) to obtain numeric macrographs. These files were thereafter subjected to the measurement of surface fractions in order to specify the quantities of oxide lost by spallation during the post-isothermal stage cooling.

Inside examination of the oxidized samples

The oxidized samples were thereafter covered with a thin layer of gold deposited by cathodic pulverization, to make these surfaces electrically conductive. These allowed depositing a thicker layer of nickel all around the samples (cathodically polarized) by electrolytic deposition in a Watts bath heated at 50°C (current density: about 1.6 A/dm^2). The samples were then cut using a Buhler Isomet 5000 precision saw, embedded in a mixture consisting in an araldite resin Escil CY230) and a hardener (Escil HY956). Polishing of the obtained mounted samples was performed with SiC-papers from 240-grade to 1200-grade, and finished by textile enriched by 1µm-alumina particles. The obtained cross-sections were examined using an optical microscope (Olympus BX51) with captures of micrographs of the external oxides scales and measurement of their average thicknesses.

Full Paper

RESULTS AND DISCUSSION

Oxidation during cooling

The cooling parts of the thermogravimetric curves also plotted in the Δm/S = f(T) scheme allow studying the progress of the eventual spallation. When no oxide is lost during cooling this part of the curve first continues to increase but more and more slowly since the thickness of the now continuous oxide layer has become important during the isothermal stage and, furthermore, the temperature decrease induces a slower diffusion though the scale. When temperature is lowered enough the mass decreases more and more rapidly because of the not-linear part of the artificial decrease in mass due to the Archimede's thrust variation. This can be clearly seen in Figure 1(a) for the cooling in dry or wet air from the 1000°C-isothermal stage. In contrast, if oxide spallation occurs during cooling the mass variation curve becomes irregular and shows a much rapid decrease in mass, as illustrated by the cooling part of the curve from 1100°C in dry air (Figure 1(b)).

The thermogravimetric curves (Figure 1, all graphs) show that oxide spallation at cooling is favored by a higher temperature of isothermal stage, and also by dry air by comparison with

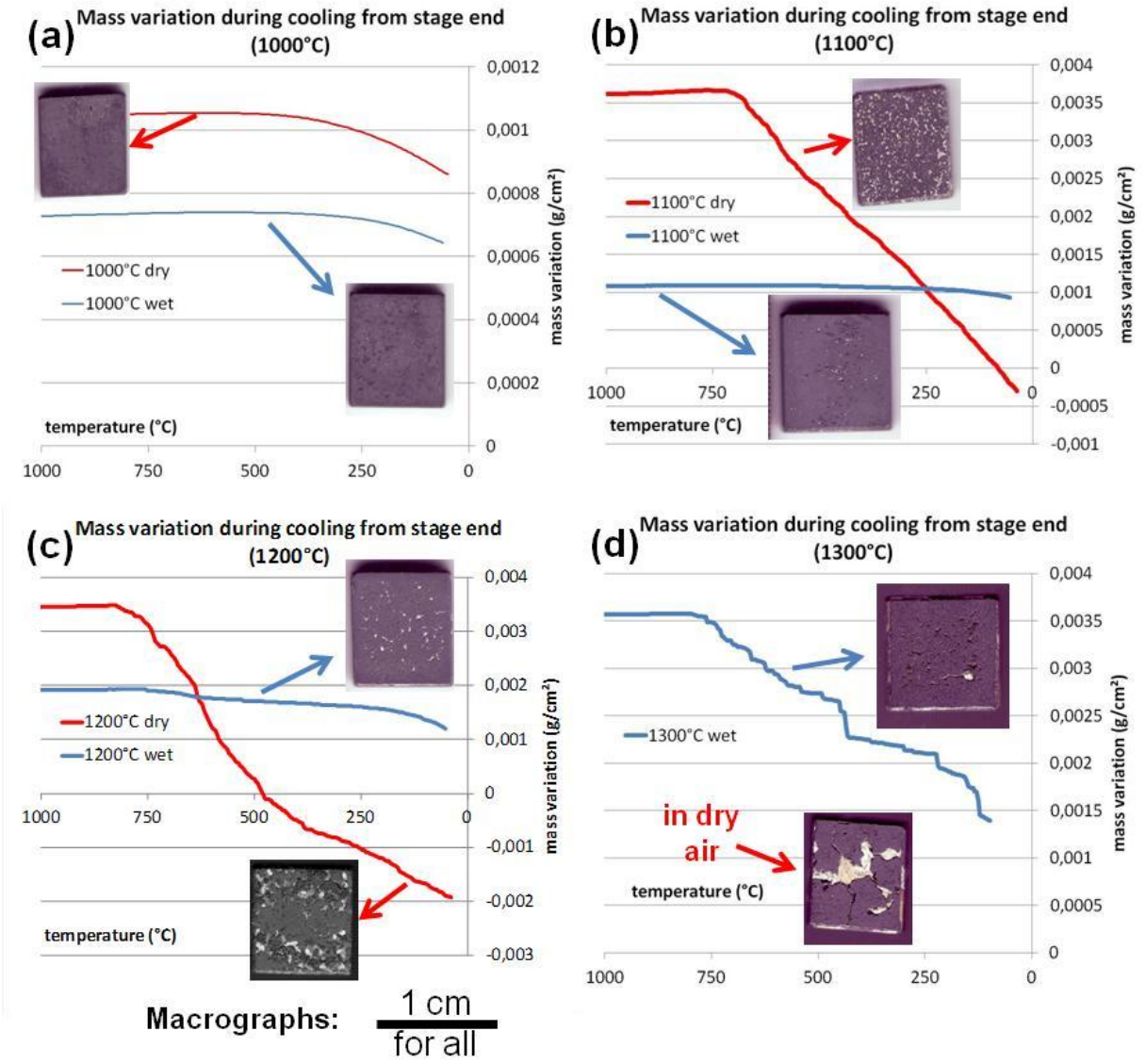

Figure 1 : Curves of mass variation of the Ni25Cr samples during cooling after oxidation in the two atmospheres

wet air. Indeed, after 48h at 1000°C the cooling does not induce any loss of oxide, neither after oxidation in dry air nor in wet air (a), which is confirmed by the surface states of the oxidized samples which are still totally covered by oxide (macrographs incrusted in Figure 1(a)). During the cooling from 1100°C the sample oxidized in wet air does not suffer from any spallation while, in contrast, the sample oxidized in dry air is affected by a continuous loss in mass, which can be thereafter interpreted by the loss of surface oxide as illustrated by the macrographs (b). For a cooling from 1200°C the sample oxidized in dry air is also affected by oxide spallation, a phenomenon which also appears for the sample oxidized at the same temperature in wet air. Here too the surface states of the samples bring confirmation (c). A real (but little) spallation phenomenon appears for the sample oxidized in wet air after an isothermal oxidation at 1300°C, as revealed by a cooling part of thermogravimetry curve now irregular (d). For the same temperature the sample oxidized at 1300°C in dry air has lost an especially great part of its external oxide scale, as demonstrated by the macrograph embedded in the graph. Unfortunately a problem with the mass gain measurement during the cooling made that the cooling part of the corresponding thermogravimetric curve is not available.

The cooling parts of the curves were further exploited by specifying the temperature levels of spallation beginning and a mass loss rate if applicable (TABLE 1). It appears that spallation begins at a temperature which is higher for a higher isothermal stage temperature for the samples oxidized in dry air (about 700°C after an isothermal oxidation at 1100°C and about 800°C after isothermal oxidation at 1200°C; data not available for 1300°C) while the temperature of spallation for the samples oxidized in wet air at 1300°C tends to be lower, confirming another time the better adherence of the oxide grown in wet air. The mass loss rates, determined as the slopes of the regression straight lines which can be drawn on the decreasing irregular parts of the corresponding curves of Figure 1, tends to be higher for a higher isothermal stage temperature in dry air, and to be much lower after oxidation in wet air.

The surface fraction measurements done by image analysis on the two main sides of the oxidized samples lead to the results given in TABLE 2. The values confirm with a quantitative dimension, the preceding observations concerning the effect of the air humidity and the temperature of isothermal stage on the amount of oxide lost by spallation at cooling.

TABLE 1 : Oxide spallation occurence at cooling (+ temperature start & rate if any) versus oxidation temperature and air humidity

	Temperature of spallation start (°C)		Average mass loss rate (µg/cm²/°C)	
air	**dry**	**wet**	**dry**	**wet**
1300°C	not applicable	788	not applicable	2.80
1200°C	838-755	/	11.9 then 3.92	/
1100°C	738-688	/	5.74	/
1000°C	/	/	/	/

TABLE 2 : Surface fraction of denuded alloy after oxide spallation during cooling (versus oxidation temperature and air humidity)

%	dry air		wet air	
air	**average**	**±std dev.**	**average**	**±std dev.**
1300°C	18.26	4.48	1.83*	1.48*
1200°C	18.08	2.19	3.45	1.56
1100°C	8.54	0.87	0.64	0.36
1000°C	0.52	0.16	0.43	0.15

***: measurements not accurate because shadow effect (the real value are much higher than the present ones)**

Metallographic characterization of the oxides scales

When observed by microscopy the oxide surfaces present different textures or reliefs. The external part of the oxide scales formed over the samples in wet air tend to be more finely structured than the ones formed in dry air, as illustrated in Figure 2 by SEM-micrographs. XRD experiments additionally show that, if chromia is

the main oxide present in the external scales, other oxides may also have formed (examples in Figure 3). In fact, NiO and Cr_2NiO_4 are effectively also present, but only for some of the samples oxidized in dry air: Cr_2NiO_4 for 1000°C, NiO, and Cr_2NiO_4 for 1100 and 1200°C. In contrast, Cr_2O_3 is the single oxide present on the surface of the sample oxidized in dry air at 1300°C, as well as on the samples oxidized in wet air whatever the stage temperature. Peaks corresponding to nickel (alloy) are also visible, because either of the low thickness of oxide (lowest stage temperatures) or of the presence of some oxide-denuded zones.

After electrolytic deposit of a nickel layer (visible in the upper part of the micrographs) to protect the surface oxide from stresses induced by the following steps of metallographic preparation, cutting and polishing, the obtained cross-sections were examined by optical microscopy. The surface states are illustrated by the micrographs presented in Figure 4. One can see that the oxide thickness increases logically with temperature. In contrast, for a given stage temperature, there is no evident dependence of the average oxide thickness on the presence of water in air. Knowing both the thickness of oxide and the surface fraction of lost oxide it was possible to calculate, using the volume mass (density) of chromia, the corresponding mass loss of oxide to compare to the mass losses deduced from the cooling part of the thermogravimetry results

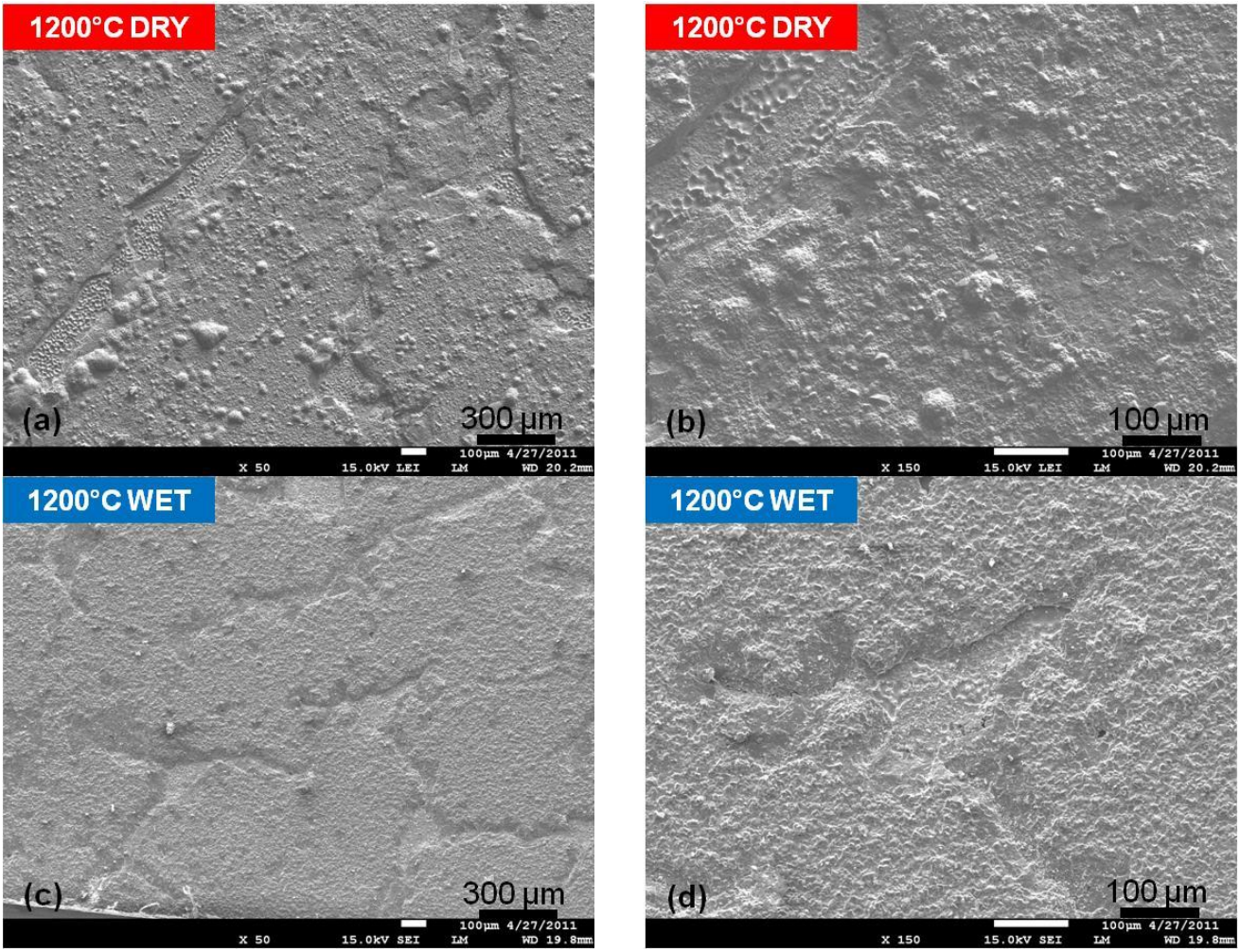

Figure 2 : Example of structure difference depending on the air humidity observed for the external oxide covering the sample before cutting (SEM macrographs, magnification: ×50 (left) and at ×150 (right))

(corrected from the artificial variation induced by the air buoyancy variation, especially rapid for medium temperatures. If the comparison between the two did not lead generally to a very good fit, the trends mentioned above were found again.

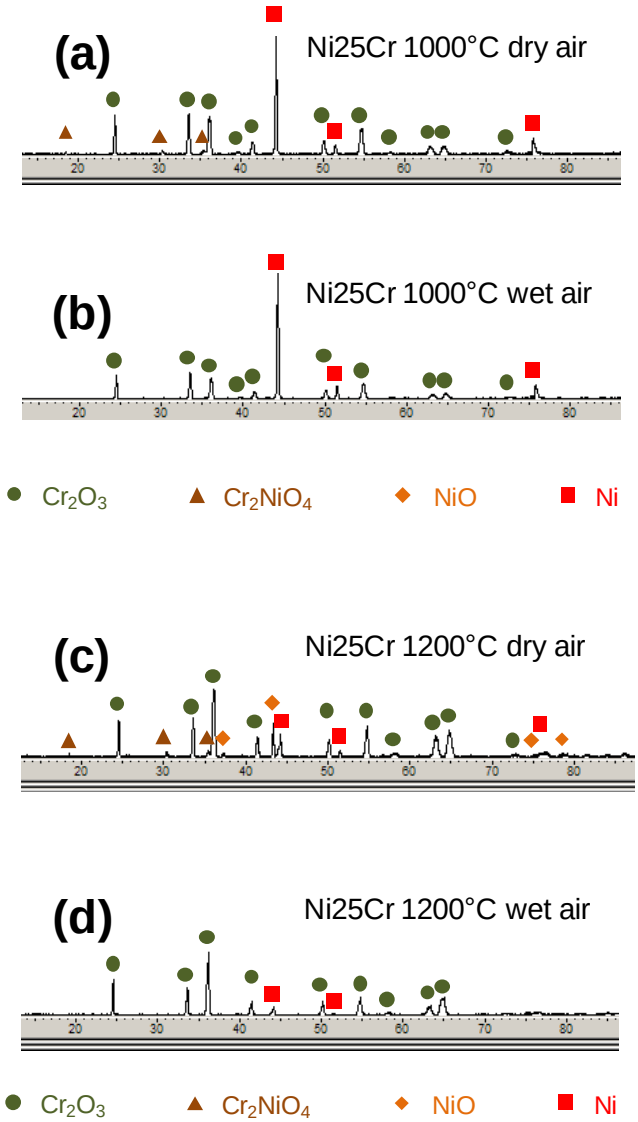

Figure 3 : Examples of results of x-ray diffraction performed on the surfaces of the oxidized Ni25Cr samples: after oxidation at 1000°C in dry (a) or wet (b) air, and after oxidation at 1200°C in dry (c) or wet (d) air

General commentaries

The cooling parts of the thermogravimetry curves may be also exploited to better characterize the spallation phenomena, deeper than the simple observation of the surface states of the samples after return to room temperature. Here, one saw that spallation is probably favoured by a higher temperature of isothermal stage, which means a thicker oxide thickness of external oxide scale after a same duration. The presence of water seems having also an effect, by retarding the spallation, even by avoiding it in some cases (oxide scale not too thick, as after 48 hours at 1000, 1100 or 1200°C). Since the thicknesses of the oxide scales do not

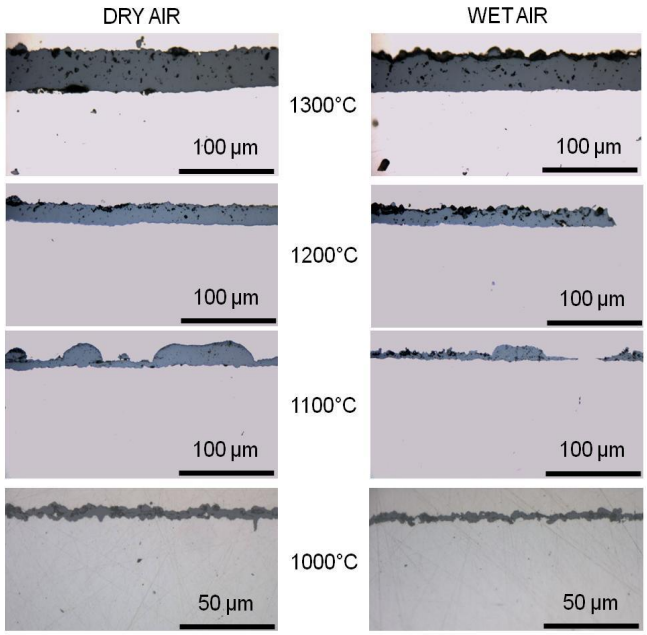

Figure 4 : External oxides scales observed in cross section on the Ni25Cr alloys after the whole oxidation tests

really depend on the presence or not of water in the atmosphere (for the range of water concentrations studied here), the explanation can be perhaps to find in the difference of nature or texture of the external oxide: it is possible that a coarser oxide, or the presence of some NiO and/or $NiCr_2O_4$ oxide, may threaten the adherence of the oxide on its substrate, or modify either its thermal expansion behaviour or its mechanical properties. The probable effect of the thickness of oxide can be further studied by performing shorter or longer isothermal stages at the same temperatures, and the spallation behaviour of the oxide formed in dry air and in wet air further

studied by trying faster or slower coolings, to better discriminate the effect of the air composition.

CONCLUSIONS

The presence of water vapour in hot air has thus also a significant influence on both the external morphology of the oxide scale isothermally developed on the alloys and its persistence on surface when temperature varies, in addition to the oxidation start when the temperature rises and to the growth mechanisms and kinetics in isothermal conditions. For the humidity tested here a better adherence was observed on the studied cast nickel-chromium binary alloy, although the inverse effect is sometimes observed for other {alloy + humidity + temperature} conditions. Further investigations will be necessary to understand this difference of behaviour by comparison with dry air, possible source of improvements for the behaviour in cyclic oxidation.

ACKNOWLEDGEMENTS

The authors thank Lionel Aranda for its help in performing the thermogravimetry tests, Ludovic Mouton for the SEM examinations, and Pascal Villeger for the XRD runs.

REFERENCES

[1] M.J.Donachie; S.J.Donachie; 'Superalloys: A Technical Guide', 2nd Edition, ASM International: Materials Park, **(2002)**.
[2] D.J.Young; 'High Temperature Oxidation and Corrosion of Metals', Elsevier, Amsterdam, **(2008)**.
[3] N.K.Othman, N.Otyhman, J.Zhang, D.J.Young; Corrosion Science, **51**, 3039 **(2009)**.
[4] B.Pujilaksono, T.Jonsson, H.Heidari, M.Halvarsson, J.E.Svensson, L.G.Johansson; Oxidation of Metals, **75**, 183 **(2011)**.
[5] E.Essuman, G.H.Meier, J.Zurek, M.Hänsel, T.Norby, L.Singheiser, W.J.Quadakkers; Corrosion Science, **50**, 1753 **(2008)**.
[6] S.Q.Zhao, X.S.Xie, J.X.Dong; Journal of Chinese Society of Power Engineering, **31(10)**, 797 **(2011)**.
[7] Y.Wu, T.Narita; Materials and Corrosion, **60 (10)**, 781 **(2009)**.
[8] P.Berthod, L.Aranda, P.Lemoine; Materials Science: An Indian Journal, **5(1)**, 42 **(2009)**.
[9] P.Berthod, L.Aranda, C.Vébert; Materials Science: An Indian Journal, **5(1)**, 49 **(2009)**.
[10] P.Berthod, A.Chiaravalle, S.Raude; Materials Science: An Indian Journal, **5(2)**, 94 **(2009)**.